ELSEVIER

Atmospheric Research 34 (1994) 85–98

ATMOSPHERIC RESEARCH

Remote sensing the susceptibility of cloud albedo to changes in drop concentration

S. Platnick[a], S. Twomey[b]

[a]*NASA Ames Research Center, M.S. 245-4, Moffett Field, CA 94035-1000, USA*
[b]*unaffiliated*

(Received December 21, 1992; revised and accepted June 10, 1993)

Abstract

The role of clouds in reflecting solar radiation to space and thereby reducing surface heating is of critical importance to climate. Combustion processes that produce greenhouse gases also increase cloud condensation nuclei (CCN) concentrations which in turn increase cloud drop concentrations and thereby cloud albedo. A calculation of *cloud susceptibility*, defined in this work as the increase in albedo resulting from the addition of one cloud drop per cubic centimeter (as cloud liquid water content remains constant), is made through satellite remote sensing of cloud drop radius and optical thickness. The remote technique uses spectral channels of the Advance Very High Resolution Radiometer (AVHRR) instrument on board the NOAA polar orbiting satellites. An approximation for the effect of the atmosphere on the signal received by the AVHRR is included in the analysis. Marine stratus clouds, as well as being important modifiers of climate, are cleaner than continental clouds an so likely to be of higher susceptibility. Analysis of several stratus scenes, including some containing ship tracks, supports this expectation.

1. Introduction

It is the *cloud sensitivity* (Arking, 1991), defined as the change in energy absorbed by the climate system to changes in a cloud parameter, that is meaningful for climate change. Important cloud parameters include the macroscopic (such as cloud amount, or cloud cover fraction, and cloud height and thickness) and the microscopic (cloud liquid water content, drop size and phase). An important cloud microphysical parameter, not typically incorporated into GCM's, is drop size. Cloud reflectance is partially dependent on drop size which is in turn linked with cloud condensation nuclei (CCN) concentrations present during cloud de-

SSDI 0169-8095(93) E0096-H

velopment. CCN concentrations are variable, having both natural and anthropogenic sources. Among the latter sources are combustion processes that also release CO_2, a major greenhouse gas. The overall effect of increasing CCN is to increase cloud albedo which results in cooling. There is no compensating outcome in the infrared (Twomey, 1977; Grassl, 1982). In light of these concerns, it is useful to define a quantity representing the *sensitivity* of cloud albedo to changes in CCN concentration. This quantity is referred to as *cloud susceptibility*. It is important to appreciate that modification of cloud albedo by CCN does not solely constitute a climate feedback. That is, the effect does not depend on the development of any actual climate change and can occur quite free from any such controversy. In the jargon of climate change, modification of drop sizes constitutes a *climate forcing* mechanism.

As expected, not all clouds are equally susceptible; the determining factors are primarily cloud optical thickness and drop size. Both can be inferred remotely through solar reflection measurements at wavelengths which are absorbing and non-absorbing for liquid water. Since global susceptibility is of importance for climate, a satellite remote sensing scheme has been developed using the Advanced Very High Resolution Radiometer (AVHRR) aboard the NOAA polar satellites. Channel 3 of the AVHRR, at 3.75 μm, provides the absorbing wavelength. Thermal emission by the cloud, and surface, at this wavelength contaminates the solar reflected signal. Brightness temperature in channel 4, in the thermal infrared, is used to estimate this emission. Similar use of the AVHRR for cloud drop size retrievals was first made by Arking and Childs (1985). This study primarily investigates maritime stratus clouds which are expected to be cleaner and so have the greatest susceptibilities to albedo modification. Results for a number of these stratus scenes are presented.

2. Cloud susceptibility

The ultimate fate for a given wavelength of the incident radiation is partially dependent on the cloud drop density (N) which ranges from tens per cm^3 for very clean air to thousands per cm^3 for continental or polluted air. The final drop density is approximately proportional to the number density of CCN present during cloud formation. Experimental data of CCN versus supersaturation (Twomey and Wojciechowski, 1969) and measurements of both CCN and N by Twomey and Warner (1969) give an approximate linear fit between CCN and drop concentration.

For critical supersaturations below 1%, the difference in CCN concentrations between continental and clean maritime air can easily be greater than an order of magnitude (Twomey and Wojciechowki, 1969). Combustion processes are also found to be an abundant source for CCN (e.g., Squires, 1966; Warner and Twomey, 1967). Hobbs et al. (1980) made measurements of elevated CCN in power plant plumes and found order of magnitude increases of cloud drop numbers in clean marine stratus effected by the plume.

Twomey (1974) discussed a link between pollution and cloud albedo. Since combustion processes are known to be prolific sources of CCN, a cloud forming in a polluted air mass will end up with a larger concentration of cloud drops than for the same cloud developing under identical circumstances in cleaner air. Optical thickness (τ) is proportional to r^2N (r is drop radius). So increases in number concentration will increase optical thickness which then leads to an increase in cloud albedo. But, it is reasonable to assume that clouds forming under the same set of circumstances but with different CCN amounts will have the same supply of vapor available for drop growth. For such a case the liquid water content ($W=4\pi Nr^3/3$ grams of liquid per cm^3) of the mature clouds can be expected to be equivalent so that drop sizes in the polluted cloud would be smaller than those for the clean cloud. The competing effect of larger N and smaller r gives $\tau \propto N^{1/3}$.

The question then arises as to the significance of the albedo change; clouds formed in clean maritime air having low CCN concentrations are more susceptible than those formed in particle-rich continental air. When A, N and ΔN are known, a calculation can be made for the change in albedo, but since ΔN is variable it is useful to define a parameter that will characterize the sensitivity of albedo to changes in drop concentration. The derivative $\mathrm{d}A/\mathrm{d}N$ (approximately equivalent to choosing $\Delta N=1$) represents such a link (Twomey 1989). Since, in general, $A=A(\tau,\bar{\omega}_o,g)$, the derivative can be expressed in the form

$$\frac{\mathrm{d}A}{\mathrm{d}N}=\frac{\partial A}{\partial \tau}\frac{\mathrm{d}\tau}{\mathrm{d}N}+\frac{\partial A}{\partial \bar{\omega}_o}\frac{\mathrm{d}\bar{\omega}_o}{\mathrm{d}N}+\frac{\partial A}{\partial g}\frac{\mathrm{d}g}{\mathrm{d}N} \tag{1}$$

and under the condition of constant liquid water content will be termed *cloud susceptibility*. Note that all terms are wavelength-dependent. Consider the special case of conservative scattering from cloud drops which, in the absence of significant graphitic carbon or other strongly absorbing aerosol, is applicable in the visible and where about one-half of solar flux occurs. There $\bar{\omega}_o=1$ and g is approximately constant with radius, so the last two terms in Eq. (1) can be neglected. Susceptibility reduces to

$$\left.\frac{\mathrm{d}A}{\mathrm{d}N}\right)_{W=\mathrm{const}}=\frac{\partial A}{\partial \tau}\frac{\tau}{3N}=\frac{4\pi\rho_l}{9W}\tau\frac{\partial A}{\partial \tau}r^3 \tag{2}$$

where either N, or r and W, can be used as independent variables (N is the more fundamental quantity but solar reflection measurements, the basis of the remote sensing scheme, contain information regarding radius only). Of obvious note is the r^3 dependence in the second form. Unless using analytic approximations, numerical calculations for $\partial A/\partial \tau$ will be needed. For a vertically inhomogeneous cloud, Eq. (2) can be applied to individual homogenous layers so that the original term $\mathrm{d}\tau/\mathrm{d}N$ can be replaced by $\Sigma\frac{\mathrm{d}\tau_i}{\mathrm{d}N}=\Sigma\tau_i/3N_i\propto\Sigma\tau_i r_i^3/W_i$, where the index i represents the different cloud layers, each with some N_i, r_i and W_i. For an instance when N is approximately constant with height, the radius and liquid water content at any layer can be used to calculate the susceptibility for the entire cloud.

The term $\tau\partial A/\partial\tau$ is given by the two stream approximation as $A(1-A)$ which has a peak at an albedo of 0.5 and an optical thickness of about 13. When multiplied by r^3 (and the term containing liquid water content) the approximation becomes susceptibility (see Fig. 1). Calculations with a detailed radiative transfer code also give a peak in susceptibility at 50% albedo for all radii. So an upper limit to susceptibility might be expected to be about 0.01 cm^3 (for $\tau=13$, $r_{\mathrm{eff}}=20$ μm and $W=0.3$ g/cm^3) and indicates that the addition of one drop per cm^3 would increase the cloud albedo by 1%. The two stream approximation can also be used to show albedo changes due to non-differential changes in drop concentration. Consider a cloud having drop concentration N. If N is changed by some factor χ (i.e., $N\rightarrow\chi N$) then $\tau\rightarrow\chi^{1/3}\tau$ and

$$\Delta A=[A(1-A)(\chi^{1/3}-1)]/[A(\chi^{1/3}-1)+1]. \qquad (3)$$

For instance, at $A=0.5$, a doubling in N will increase albedo to a value of 0.56. Similar to susceptibility, the peak in ΔA occurs very close to $A=0.5$ for reasonable χ (<2).

The important point is that existing cloud microphysics is essential in determining the climate forcing by CCN. Climatologies of cloud albedo may be adequate for understanding the current short-wave energy balance, but *are not* sufficient for estimating changes in the energy balance; cloud microphysics must also

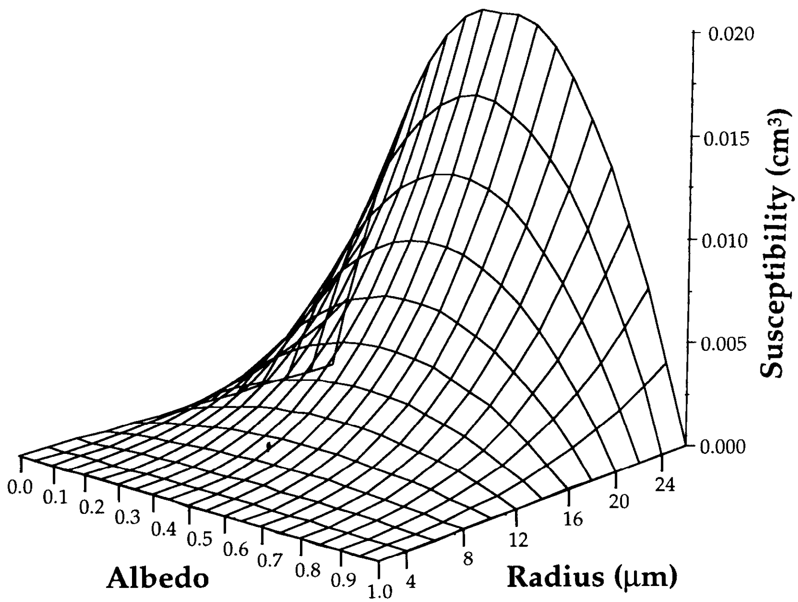

Fig. 1. Calculated surface of susceptibility versus radius and albedo, using the two stream approximation with a liquid water content of 0.3 g/m^3.

be known. Climate modeling of this effect typically assumes that drop concentrations in clean maritime clouds increase by some factor. While changes in other climate modifiers, such as CO_2, may be usefully expressed in this way, the same is not true of drop concentration. For example, pollution is more likely to increase CCN concentrations by some absolute number, say 10 cm^{-3}, over some geographical region. The effect on a cloud that would otherwise have drop concentrations of 10 cm^{-3} can be very different than for a cloud having the same albedo but with $N = 100$ cm^{-3} (and a smaller geometrical thickness). Each will respond differently to the increase in drop concentration (see Eq. 3). It is not at all clear that every maritime cloud should have about the same drop concentration, which is one of the underlying assumptions of using a factor increase in N to model albedo modification. So, in addition to albedo, drop concentration must be known, and simple assumptions about the microphysics can be misleading. Any figure of merit for susceptibility will have a two dimensional functional dependence that will include albedo (or optical thickness) and a microphysical variable (e.g., A and N, A and r, τ and r, A and χ); the exact definition is largely irrelevant.

Pollution is also a source of carboniferous aerosol which absorbs in the visible. This effect on cloud albedo, considered by Twomey (1977) and Grassl (1982), can only be seen in the brightest clouds. This is in agreement with AVHRR studies by Kaufman (1993) of cloud reflectances in the Brazilian Amazon basin in the presence of dense smoke which showed a reduction in the visible albedo for initially bright clouds (from 0.71 to 0.67) along with expected reduced drop sizes. However, the process defined by susceptibility, which only accounts for the CCN effect, is likely to be the dominant radiation influence of particulate pollution for relatively clean maritime clouds far from intense sources. It should be added that susceptibility also doesn't account for the effects of meteorology and chemistry on the development, nucleation and lifetime of CCN.

3. Remote sensing susceptibility

Inferring drop radius through near infrared absorption has been used by a number of investigators (e.g., Twomey and Cocks, 1982; Stephens and Platt, 1987) using aircraft borne sensors. None of the investigators made measurements in the 3.75 μm window. In situ cloud measurements typically showed that drop radius was overestimated by 2 μm to 5 μm. Retrieving larger drops implies that the observed $\bar{\omega}_0$ is lower than would be expected from calculations based on measured drop sizes. This has been termed anomalous absorption. Stephens and Tsay (1990) give a review of the measurements and comment on proposed causes of the anomaly. Suggested causes include continuum vapor absorption in the windows and cloud inhomogeneities. It is not clear whether radius inferred from a 3.75 μm channel would suffer from a similar anomaly. The much larger liquid water absorption 3.75 μm (order of magnitude greater than at 2.2 μm) might tend to mask out any unaccounted for continuum vapor absorption. The large liquid water absorption also suggests that the mean number of scatterings for reflected photons would be small and photon penetration into the cloud, both vertically and horizontally, would be reduced implying that the effect of inhomogeneities would be less. For example, consider a cloud with 10 μm drop radii and $\mu_o = 0.85$. Our Monte Carlo calculations show about 8 mean scatterings for reflected photons at an optical thickness of 10 versus 20 mean scatterings in the visible. The rms horizontal displacement for 3.75 μm reflected photons reaches an asymptotic limit of about 6 optical path units for a cloud optical thickness about 10 or greater. For comparison, in the visible the rms displacement is 13 optical path units for a cloud optical thickness of 10 and an optical displacement of 18 when optical thickness is 20. In the vertical, maximum 3.75 μm photon penetration can be approximated by the optical thickness at which the reflection reaches its asymptotic value — about 4 to 7 for 20 μm and 6 μm drop radii respectively. Jonas (1992) made Monte Carlo calculations at visible and 3.9 μm wavelengths for clouds with cellular structures. His calculations also show the effect of inhomogeneities to be reduced at the more absorbing wavelength. Comparative curves of albedo in the visible, at 3.75 μm, and at other window wavelengths are shown in Fig. 2 for $r_{\text{eff}} = 10$ μm.

Quantitative retrievals of cloud drop radii and optical thickness using the 3.75 μm window on the AVHRR were first made by Arking and Childs (1985). Grainger (1990) used the AVHRR for studying orographic effects on drop sizes and optical thickness. No in situ cloud measurements were used for validation in either study. Qualitative studies of ship tracks using the AVHRR include Coakely et al. (1987) and Radke et al. (1989). Emission at 3.75 μm is comparable to, and can

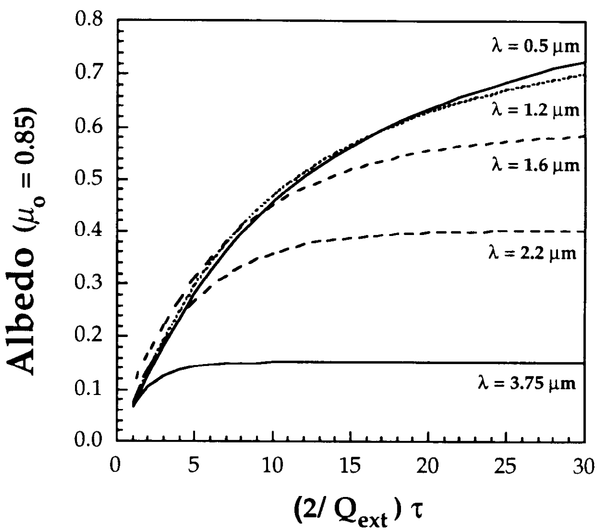

Fig. 2. Cloud albedo as a function of optical thickness for five window wavelengths. Drop radius is 10 μm for each curves and the cosine of the solar angle, μ_o, is 0.85.

even exceed the reflected radiation. Fig. 3 shows the ratio of reflected solar radiation to emission in AVHRR channel 3 when both cloud and surface have a temperature of 290 K. The two intensities are seen to be equal for drop radii of about 10 μm. Calculations of both reflectance and emission where made using the doubling/adding technique of Twomey et al. (1966). While removing emission is certainly an added complication, the large absorption in the channel does give its use one very important advantage — the signal is almost entirely dependent on radius, with very little optical thickness sensitivity except for the thinnest clouds. Shorter wavelengths have substantial optical thickness dependencies over much of the expected radius range. The substantial radius information content of a 3.75 μm channel makes it of special interest for remote sensing regardless of it being a major contender for cloud microphysical studies.

Inferring optical thickness and drop radius from satellite reflection and emission data characterizes an *inverse* problem which, in this study, is determined by the best fit between the satellite measurement and *forward* calculations placed into a library file. The library contains bidirectional reflectances for AVHRR channels 1, 2 and 3 (at 0.65, 0.85 and 3.75μm respectively) and effective cloud and surface emissivities for channels 3, 4 and 5 (the latter two channels at about 10.75 and 12.0 μm, respectively). The contents of the library includes calculations for radii equal to 1, 4, 6, 8, 10, 12.5, 15, 17.5, 20, 25, 30, 35 and 45 μm.

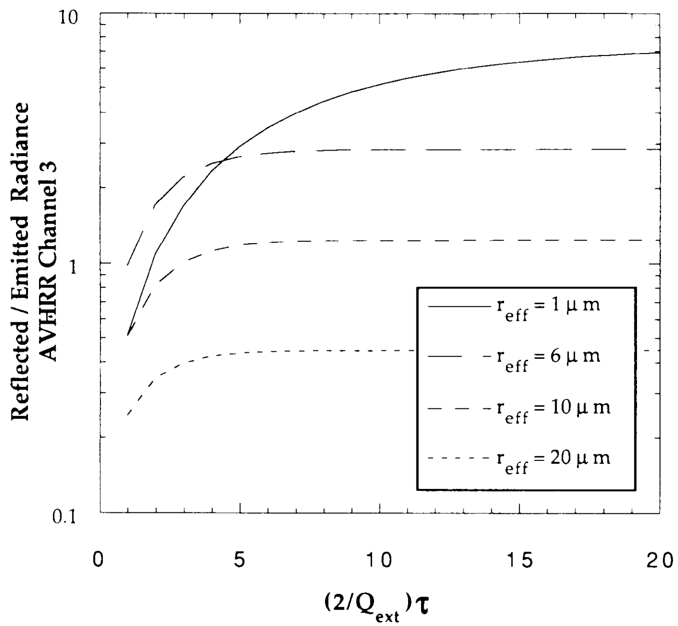

Fig. 3. The ratio of reflected solar intensity to thermal emission for AVHRR channel 3 as a function of optical thickness for four drop radii. Surface and cloud temperatures are both 290 K. The azimuthal average is used for reflection with $\mu_o = 0.75$ and $\mu_{sat} = 0.85$.

These radii are the mean of a normal distribution with a dispersion of 0.2 (giving $r_{eff} \approx 1.08 r_{mean}$). The surface, assumed to be the ocean for this study, is considered Lambertian to diffuse radiation with albedos of 0.06, 0.03, 0.01, 0.0 and 0.0 for channels 1 through 5 respectively. Variations in radiative properties over the finite band of each AVHRR channel is considered in the calculations. In practice, only channels 1, 3 and 4 were needed. Channel 5 was used with channel 4 in a split window technique for inferring sea surface temperature. The error functions used in the comparison of library entries with satellite data show a well defined and unique minimum when radii of 1 μm are excluded from the solution set. The effect of the atmosphere on the signal received by the satellite was approximated using the LOWTRAN7 radiation code (Kneizys et al., 1988).

Channels 1 and 2 lack onboard calibration and must, without in-flight techniques, rely on calibrations typically performed several years before launch. In-flight calibrations with scenes of known reflectance shows that the sensor response is modified from the pre-flight calibration (see Teillet et al. 1990). All NOAA-11 channel 1 and 2 data in this study uses the calibration coefficients of Che et al. (1991). The in-flight calibration made closest in time to the recording of the data being studied is chosen. NOAA-9 and -10 AVHRR data is calibrated in the same way with the Teillet et al. gain values. These in-flight calibrations are made in terms of a reflected intensity. This is converted to albedo using the solar flux data of Neckel and Labs (1984).

A detailed discussion of each topic in this section can be found in Platnick (1991).

4. Results

A common difficulty in satellite remote sensing is comparison with in situ measurements. As part of the First ISCCP Regional Experiment (FIRE), field observations were made of marine stratocumulus clouds off the coast of southern California in the summer of 1987. Two reports have been published of cloud microphysical measurements taken at times almost concurrent with the pass of a NOAA polar orbiter.

The aircraft measurements by Rawlins and Foot (1990) were taken over the course of several hours on the afternoon of 30 June 1987. Additional data from this flight was obtained from the Meteorological Research Flight of the UK Meteorological Office (Taylor 1991, private commun.). A run was made within and above a 300 meter thick cloud. Effective radii of about 9.0 μm were calculated from drop size distributions near cloud top. Optical thickness, estimated from their cloud reflectance data, varied from 15 to 60. We analyzed a NOAA-9 AVHRR LAC image acquired within an hour of the aircraft measurements, for a north–south flight path flown by the plane. In this region, $\mu_o \approx 0.90$ and $\mu_{sat} \approx 0.50$ (corresponding to a pixel resolution of about 3.8 km). Fig. 4 shows our retrievals giving radii of 10 μm along the entire path with one pixel showing 8 μm; optical thickness varies from 20 to 70. Agreement between retrieved values of radius and

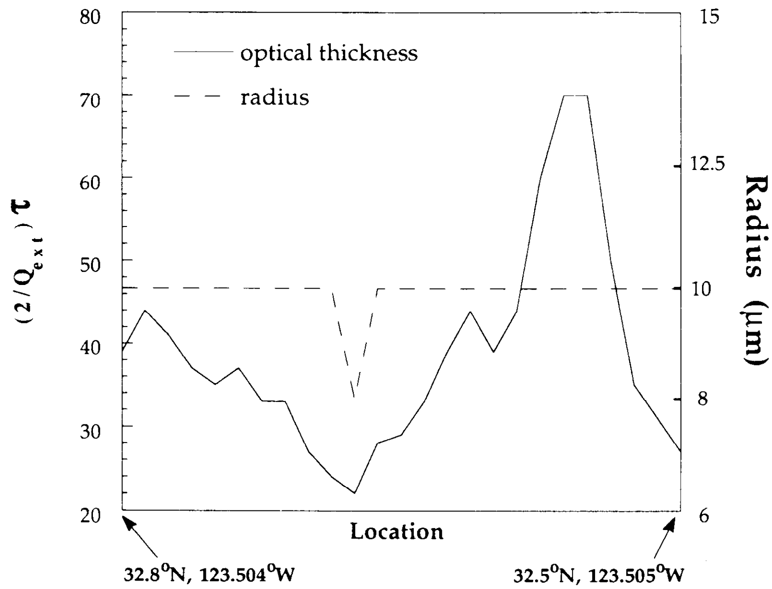

Fig. 4. Radius and optical thickness retrieved from a NOAA-9 LAC image, 30 June 1987, along an aircraft flight path taken by Rawlins and Foot (1990) in stratocumulus off southern California.

the in situ measurements are within the radius increments available from the library data (at a radius of 10 μm, increments of +2.5, −2.0 μm in radius are possible to resolve with the library). Radius was not sensitive to the specific atmospheric correction. Susceptibilities, using Eq. (2) normalized to a typical cloud liquid water content of 0.3 g/m^3 (used in all susceptibility calculations that follow), vary over an order of magnitude, from about 0.5×10^{-3} at the northern end of the cloud region to as high as 6.0×10^{-3} at the southern end (units of cm^3 will be assumed throughout this paper).

Radke et al. (1989) reported passage through two ship tracks within a stratocumulus cloud layer on 10 July 1987. Radiation and microphysical measurements were taken midway between the approximately 500 meter thick cloud. Drop concentrations were seen to increase from 30 to 50 cm^{-3} outside the track to over 100 cm^{-3} within the track, indicative of larger CCN numbers. We obtained an HRPT NOAA-10 image for this region ($\mu_o\approx0.50$, $\mu_{sat}\approx0.79$ giving about 1.7 km pixel resolution) that was captured twenty minutes before the aircraft measurements were made. Cloud parameters were retrieved along two section lines crossing the tracks. The average retrieved radius, both in and out of the tracks, was typically 3 μm to 6 μm larger than in situ measurements. Microphysical studies in California stratus typically show increasing drop sizes with height (e.g., 3 to 4 μm increase reported by Noonkester, 1984; about a 3 μm increase by Rawlins and Foot, 1990). At the 3.75 μm wavelength, absorption is larger and therefore drop sizes near cloud top contribute a greater influence to the inferred sizes than drops further down in the cloud where in situ measurements were taken. But a one to two μm difference between mid-cloud and cloud top radii can only partially explain the larger retrieved radii. Retrieved susceptibilities are smaller for the ship tracks as expected; 0.5×10^{-3} in-track and 1.0×10^{-3} to 2.0×10^{-3} out-of-track. Susceptibility calculated from the aircraft measurements is similar with 0.20×10^{-3} to 0.65×10^{-3} in-track and 0.70×10^{-3} to 1.45×10^{-3} out-of-track.

Wintertime fog in the central valleys of California is expected to be at the other end of the susceptibility scale, providing another check of the retrieval algorithm. The extensive fog forms in air containing large CCN concentrations from agricultural, industrial and natural sources. Three NOAA-11 GAC images of valley fog from the winter of 1989/90 were analyzed. Retrieved radius is especially uniform throughout the length of the valleys, typically 6 μm to 8 μm — smaller than for marine stratus as expected and in general agreement with the results of Garland (1971). Optical thickness ranged from 10 to over 100 (larger thickness found in the northern part of the Central Valley). Susceptibility was as low as 0.05×10^{-3}, two orders of magnitude less than the larger values found in California marine stratus. This is probably a lower limit since liquid water content is likely to be less than the 0.3 g/m^3 used in the calculation.

Stratus containing ship tracks is expected to have large variations in susceptibility over a small scale, providing a useful test for sensing relative susceptibility; the solar and satellite viewing angles, cloud temperatures, surface properties and atmospheric influences are similar and so relative retrievals of cloud parameters are more credible then comparisons between distant regions. A dramatic instance of ship tracks was seen in an HRPT NOAA-11 image from 2 March 1990 in a large region centered near 52°N, 140°W. Tracks were seen to be forming in uniform stratus to the west as well as in a thinner stratus region in the center of the image. Resolution was from one to two kilometers. A number of locations in the image have been analyzed including thirteen individual tracks; optical thickness and radius retrievals are summarized in Fig. 5 clearly showing smaller radii and larger optical thicknesses in the tracks. Three to five adjacent pixels were typically used to calculate the averages, designated by a single data point. Out-of-track retrievals are taken from the uniform western stratus only. A histogram of susceptibility is shown in Fig. 6. Tracks in the thinner stratus show the smaller susceptibilities and smaller optical thicknesses; retrieved radii are about the same for both region of tracks.

Marine stratus is quite common, especially near the western coasts of the continents. Two NOAA-11 GAC images in the South Atlantic, off the coast of Namibia and South Africa (4 January 1989 and 19 April 1989 with resolution of 5 to 6 km), were analyzed. Both clouds were extensive and isolated. Retrievals gave 6.0 μm to 9.0 μm radii, optical thicknesses from 3 to 12, and susceptibilities from 0.2×10^{-3} to 0.8×10^{-3}. It is impossible to make any climatological conclusion regarding the microphysics of this stratus, but for the two cases studied, radii and susceptibilities are much less than those typically found in uncontaminated California stratus. This is in contradiction to the general expectation that clouds in this hemisphere should have relatively small droplet concentrations and corre-

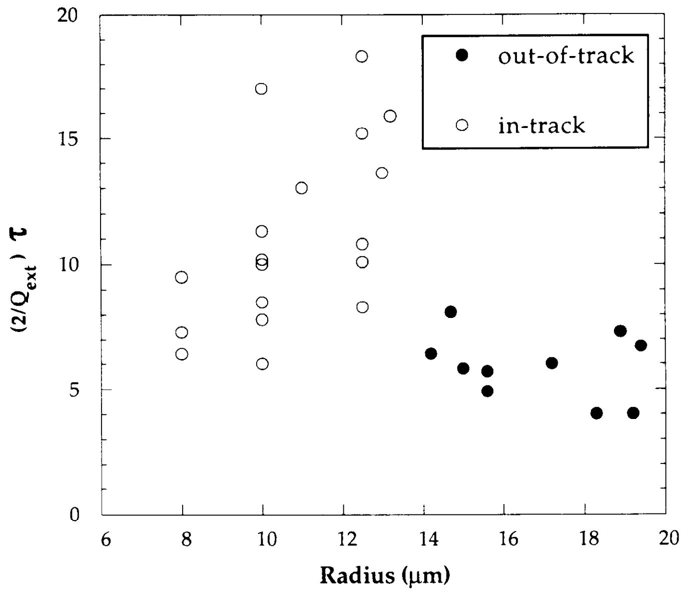

Fig. 5. Scattergram of retrieved radius and optical thickness in a stratus cloud containing ship tracks. From NOAA-11 HRPT, 2 March 1990.

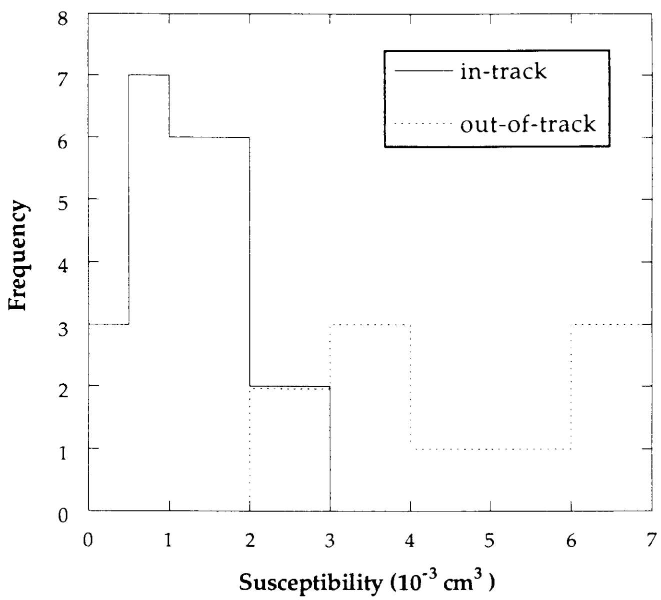

Fig. 6. Histogram of susceptibility for the retrievals of Fig. 5.

spondingly large susceptibilities. Either large CCN concentrations are found here or the liquid water content of the clouds are much smaller (by a fraction of about 0.15 to 0.30). If these results were generally true, it might explain the lack of ship track sightings in this region even though stratus development is common. A NOAA-11 GAC from 22 January 1989 was analyzed for a region south of Madagascar in the Indian Ocean (33.3°S, 45.71°E). Satellite viewing angles are near nadir giving 4 km resolution. Two likely ship tracks were seen formed in a broken stratocumulus deck. There is an obvious reduction in drop size in the apparent tracks (8 μm versus 12.5 μm to 17.5 μm for out-of-track regions) and larger optical thicknesses (8 to 15 versus 3 to 12 out-of-track). Susceptibilities are also consistent with the expectations for ship tracks, and are comparable to those found in California stratus (to the authors' knowledge, this would be the first report of ship tracks being found in the Southern Hemisphere).

5. Conclusions

The retrieved range of susceptibilities (in units of cm^3 and normalized to a liquid water content of 0.3 g/m^3) for the marine clouds studied varied by about two orders of magnitude; from as low as 0.23×10^{-3} in stratus off the west coast of southern Africa to about 20×10^{-3} in thin stratus off the California coast. Susceptibilities for California valley fog were as low as 0.05×10^{-3}, extending the measured range, for all clouds studied, to almost three orders of magnitude. A

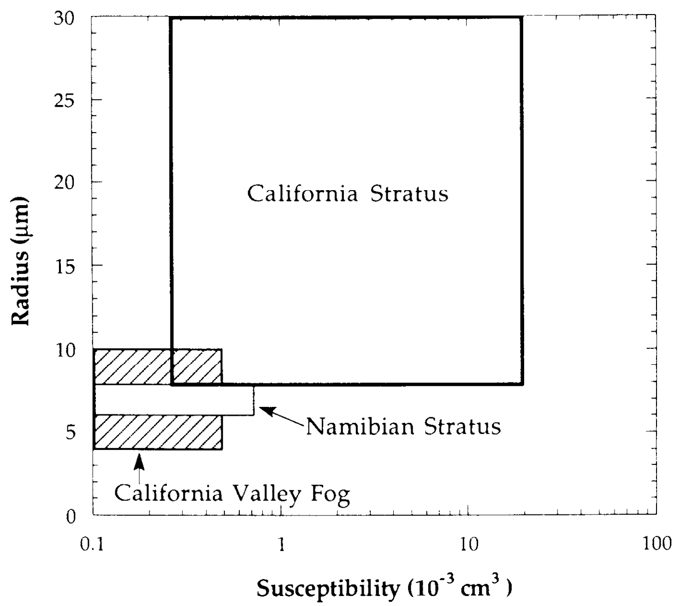

Fig. 7. Summary for the range of drop radius and cloud susceptibility retrieved during this study.

schematic summary of retrieved radius and susceptibility is shown in Fig. 7. Studies in ship tracks have shown that the tracks are indeed less susceptible than out-of-track regions after having been contaminated with CCN originating from the ship's effluent. Susceptibility, in and out of the tracks, differs by a factor of 2 to 4 and up to as high as 30 for thin stratus. The use of susceptibility extends beyond fog and marine stratus which have been highlighted in this study because of their relative homogeneity for remote sensing purposes.

Acknowledgment

This work was supported by NSF grant ATM-8716637 through the Institute of Atmospheric Physics, Tucson, Arizona.

References

Arking, A. and Childs, J.D., 1985. Retrieval of cloud cover parameters from multispectral satellite images. J. Clim. Appl. Meteorol., 24: 322–333.
Arking, A., 1991. The radiative effects of clouds and their impact on climate. Bull. Am. Meteorol. Soc., 71: 795–813.
Che, N., Grant, B.G., Flittner, D.E., Slater, P.N. and Biggar, S.F., 1991. Results of calibrations of the NOAA-11 AVHRR made by reference to calibrated SPOT imagery at white sands. In: SPIE Proc. V1943-21, Orlando, Florida.
Coakley, J.A., Bernstein, R.L. and Durkee, P.A., 1987. Effect of ship-stack effluents on cloud reflectivity. Science, 237: 1020–1022.
Garland, J.A., 1971. Some fog droplet size distributions obtained by an impaction method. Q. J. R. Meteorol. Soc., 97: 483–494.
Grainger, R.G., 1990. The Calculation of Cloud Parameters from AVHRR Data. Ph.D. Diss. Univ. Auckland, New Zealand.
Grassl, H., 1982. The influence of aerosol particles on radiation parameters of clouds. Idöjárás, J. Hung. Meteorol. Serv., 86.
Hobbs, P.V., Stith, J.L. and Radke, L.F., 1980. Cloud-active nuclei from coal-fired electric power plants and their interaction with clouds. J. Appl. Meteorol., 19: 439–451.
Jonas, P.R., 1992. Effects of variations of cloud microphysical properties on cloud reflectance. Proc. 11th Int. Conf. Clouds Precipitation, Montreal, Canada, pp. 807–810.
Kaufman, Y.J. and Nakajima, T., 1993. Effect of amazon smoke on cloud microphysics and albedo — Analysis from satellite imagery. J. Appl. Meteorol., 32.
Kneizys, F.X., et al., 1988. Users Guide to LOWTRAN 7. AFGL-TR-88-0177.
Neckel, H. and Labs, D., 1984. Solar radiation between 3000 and 12500 Å. Sol. Phys., 90: 205–258.
Noonkester, V.R., 1984. Droplet spectra observed in marine stratus cloud layers. J. Atmos. Sci., 41: 829–845.
Platnick, S., 1991. Remote Sensing the Susceptibility of Cloud Albedo to Changes in Drop Concentration. Ph.D. diss. Univ. Arizona, Tucson, Arizona.
Radke, L.F., Coakley, J.A. and King, M.D., 1989. Direct and remote sensing observations of the effects of ships on clouds. Science, 246: 1146–1149.
Rawlins, F. and Foot, J.S., 1990. Remotely sensed measurements of stratocumulus properties during FIRE using the C130 aircraft multi-channel radiometer. J. Atmos. Sci., 47: 2488–2503.
Squires, P., 1966. An estimate of the anthropogenic production of cloud nuclei. J. Rech. Atmos., 2: 297–308.

Stephens, G.L. and Platt, C.M.R., 1987. Aircraft observations of the radiative and microphysical properties of stratocumulus and cumulus cloud fields. J. Clim. Appl. Meteorol., 26: 1243–1269.
Stephens, G.L. and Tsay, S., 1990. On the cloud absorption anomaly. Q. J. R. Meteorol. Soc., 116: 671–704.
Taylor, J., pers. commun., 1991. Meteorological Research Flight, Farnborough, Hamshire, GU14 6TD, England.
Teillet, P.M., Slater, P.N., Ding, Y., Santer, R.P., Jackson, R.D. and Moran, M.S., 1990. Three methods for the absoluted calibration of the NOAA AVHRR sensors in-flight. Remote Sensing Environ., 31: 105–120.
Twomey, S., Jacobowitz, H. and Howell, H.B., 1966. Matrix methods for multiple scattering problems, J. Atmos. Sci., 23: 101–108.
Twomey, S. and Warner, J., 1967. Comparison of measurements of cloud droplets and cloud nuclei. J. Atmos. Sci., 24: 702–703.
Twomey, S. and Wojciechowski, 1969. Observations of the geographical variation of cloud nuclei. J. Atmos. Sci.: 26. 684–688.
Twomey, S., 1974. Pollution and the planetary albedo. Atmos. Environ., 8: 1251–1256.
Twomey, S., 1977. The influence of pollution on the shortwave albedo of clouds. J. Atmos. Sci., 34: 1149–1152.
Twomey, S. and Cocks, 1982. Spectral reflectance of clouds in the near-infrared: Comparison of measurements and calculations. J. Meteorol. Soc. Jpn., 60: 583–592.
Twomey, S., 1989. Aerosols, cloud physics and radiation. Plenary Lecture 3, Am. Assoc. Aerosol Res. Annu. Meet., Reno NV.
Warner, J. and Twomey, S., 1967. The production of cloud nuclei by cane fires and the effect on cloud droplet concentration. J. Atmos. Sci., 24: 704–706.